International Journal of Chemistry; Vol. 7, No. 2; 2015
ISSN 1916-9698 E-ISSN 1916-9701
Published by Canadian Center of Science and Education

Study Self-cleaning of Congo Red from Cotton Fabric Loaded by Zno-Ag

Amjed M. Oda[1], Hameed H. Ali[2], Abbas J. Lafta[3], Hussein A. Esmael[3], Ali A. Jameel[1], Abbas M. Mohammed[1], Inas J. Mubarak[3]

[1]University of Babylon, College of Basic Education, Iraq

[2]Kufa University, College of Science, Iraq

[3]University of Babylon, College of Science, Iraq

Correspondence: Abbas J. Lafta, University of Babylon, College of Science, Iraq. E-mail: abbaslafta2009@yahoo.com

Received: March 30, 2015 Accepted: April 30, 2015 Online Published: July 6, 2015

doi:10.5539/ijc.v7n2p39 URL: http://dx.doi.org/10.5539/ijc.v7n2p39

Abstract

The current work involves modification of zinc oxide by doping silver, this was achieved by photodeposition method. Modified zinc oxide was investigated using X-ray diffraction (XRD), fourier transform infrared spectroscopy (FTIR) and scanning electron microscopy (SEM). Both of ZnO and Ag doped ZnO was fabricated on a cotton texture. The photocatalytic activity of these materials was investigated by following the decolorization of congo red from simulated industrial wastewater. The decolorization of congo red over fabricated-ZnO-Ag was more efficient in comparison with non- fabricated catalysts. Different reaction parameters were undertaken including the effect of pH of the solution, irradiation time and the effect of light intensity. Complete dye removal over fabricated materials took three hours while it took 4.5 for non-fabricated materials.

Keywords: Zinc oxide, congo red dye removal, fabricated zinc oxide

1. Introduction

Photocatalytic reactions were emerged more than forty years ago when Fujishima and Honda reported photocatalytic splitting of water on titanium dioxide electrode (Manoj , Shaji and Santhosh, 2012). This type of reactions is based on the photoexcitation of the particles of the phtocatalyst with light of energy that is equal to greater than its bandgap (Eg) (Hind, Baha, Hussein, Ahmed, and Saba, 2013). This process produces valence band holes (h^+_{VB}) as well as conduction band electron (e^-_{CB}) (Narendra, Oza, and Ingale, 2014). The positive holes normally diffuse to the surface and act as a trap for hydroxyl groups, while conduction band electrons interact with adsorbed oxygen on the surface of the photocatalyst(Rizzo, Meric, Guida, Kassina, and Belgiorno, 2009). Generally, the first step in the heterogeneous photocatalytic reactions for the organic and inorganic compounds is the producing excited state of photocatlyst upon absorbing a light with a proper energy (Agustin, and Gonzalez, 1988). The second step is the de-excitation of the photocatalyst via diffusion of charge carriers into the surface and then reacting with the pre-adsorbed species on the surface (Alan, and Desmond, 11991) . In case of absence of redox species on the surface, these e^-_{CB} and h^+_{VB} are recombined together in a recombination process (Ghaed, Hossaini, and Ramezanis, 2012) (Gunnar, Niklasson, and Claes, 2007). However, presence of oxygen is very essential to perform this type of reactions as it act as trap for conduction band electron under this circumstances oxygen works as an oxidant and generate some of reactive radical species such as O_2^{-} O^- , and O_3^- on the surface (Gopel, Rocker, and Feierabend, 1983). These active radicals contribute in the initiation of photocatalytic reactions that are proceeded on the surface (Henglein, 1982).

The activity of the photocatalytic reactions can be enhanced by addition of some inorganic species such as H_2S_2 and H_2O_2 (Malinda, Reichert, Chia, and Javier, 2014). Generally, backelectron transfer can reduce the activity of the photocatalyst so the main challenge in this context is how to reduce the rate of recombination reaction which leads consequently to improve the activity of the photocatalyst. This aim can be conducted by surface modification. This can be done by some methods such as metal deposition, coupled of semiconductors, and surface sensitization, and metal and non-metal deposition(Noriyuki, Osamu, and Youkoh, 1995). Metal deposition can lead to improve the photocatalytic activity of the photocatalyst by altering some of chemical and

physical properties of the surface, increasing surface area, electrical conductance and reducing the rate of recombination reaction by acting as a sink for collection of conduction band electrons (Amy, Guangquan, and John, 1995). In the last few decades and as a result of high levels of pollution, photocatalytic reactions were applied in the pollution treatment. Among different types of pollution, pollution with dyes is an important type as these dyes are used in many applications in our modern life (Santos, Azevedo, Annar, and Dezottil, 2006). Dyes are essential type of water pollutants especially industrial water and wastewater that are charged from different factories especially from textile factories, food industries, papers and fibers industries (Zheng, Dillon, Eugen, and Albert, 2013). In this type of pollution, decolorization is the first step in the treatment and this can be performed using photocatalytic degradation of the polluted dye. This can lead to fully decontamination of the polluted dyes in to inorganic species such as CO_2, H_2O and other inorganic species (Hadjivanov, Lamotte, and Lavallery, 1997).

The present study describes the removal of congo red from the simulated industrial wastewater using the concept of the photocatalytic reactions using a suspension of both bare and doped zinc oxide with silver. These two photocatalysts were used with and without cotton fabric structure.

2. Experimental Part

2.1 Used Dye

The dye that was used as a model for the polluted dye was congo red, it is molecular formula ($C_{32}H_{22}N_6Na_2O_6S_2$). It has molar mass of 696.665 g/mol with a melting point of 360 °C and its molecular structure is shown in Figure 1(Rajeev, and Shalini, 2008).

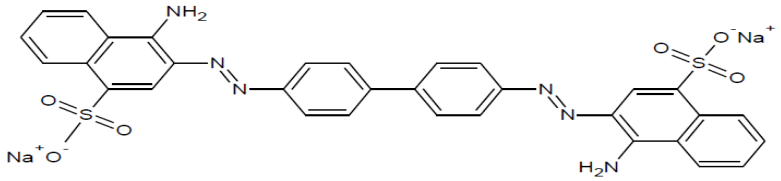

Figure 1. Molecular structure of congo red dye that was used in this study

2.2 Zinc Oxide

Zinc oxide that was used in this study was provided with Fluka company (99.5%) , its molecular formula is ZnO with a molar mass of 81.401 g/mol with a density of 5.606 g/cm3 and has a melting point of 1975 °C with a bandgap energy of 3.37 eV (Zhong, 2004).

2.3 Modification of Zinc Oxide Surface

Doping of silver on zinc oxide surface was performed using 50 mL aquous solution of 0.1 molar of silver nitrate (BDH, 99%), this mixture was irradiated with UV radiation using a Candle (5 watt.) with contineous stirring at 25 ℃. This mixture was agingated for 30 min and the balck colloidal of silver metal appeared and no silver ion precipitated as AgCl after irradiation. ZnO (Fluka company, 99.5%) 5 g was mixed with silver colloidal solution, this was stirring for 1 hour at 25 ℃ in air atmosphere. Then the proposed preciptate of Ag/ZnO was filtrated off and washed with ethanol several times and then dried at 80-100 ℃ for overnight. To prepare silver doped zinc oxide, ZnO was added to a mixture of water and acetone (50:50). The resultant suspension was mixed for one hour than silver nitrate 2.5 % of zinc oxide was added to the above mixture, this mixture was stirred under irradiation with light from low pressure mercury lamp (125 watt) for four hours under normal air. Then the solvent was evaporated at 80 °C and the resultant solid was dried under vacuum for overnight. The resultant modified Ag/ZnO was investigated using powder x-ray diffraction (PXRD), Fourier transform infrared spectroscopy (FTIR) and scanning electron microscopy (SEM).

2.4 Preparation of Cotton Fabric Loaded by ZnO-Ag

A piece of cotton wool of 10 x 10 cm was taken in this wok, this was washed and dried carefully to be ready for use in this study. Then it was immersed in the used suspension with continuous stirring to ensure loading of the catalyst on the cotton wool. Then it washed with distilled water sometimes to remove weakly adsorbed particles of the catalyst and then dried to be ready for use.

2.5 Powder X-rays Diffraction (PXRD)

The XRD patterns for both neat and silver doped zinc oxide were investigated using Simadzu-6000 X-ray diffractometer with a nickel filter using monochromatized CuKα radiation at 40 kV and it was operated at 30 mA.

The films were scanned at 2° (2θ) per min. and the scan range was 20° 2θ to 60° 2θ. The intensity was recorded with a chart speed of 25 mm/min**.**

2.6 Fourier Transform Infrared Spectroscopy (FTIR)

Functional surface groups of both naked ZnO and that modified with silver were investigated with Perkin Elminer Spectrophotometer. Before run, all the samples were grounded with KBr with a ratio roughly 1/50 of the used samples. All the samples were measured in the range of from 450 to 4000 cm^{-1} with a resolution power of 1 cm^{-1} for each scan.

2.7 Scanning Electron Microscopy (SEM)

The surface morphology of neat and silver doped ZnO was studied using Scanning Electron Microscope Inspect 550, Netherland (SEM). This machine was operated at 25 kV and derided samples of both ZnO and Ag/ZnO were adhesive on carbon tape attached to aluminum – stubbed sputter coated with platinum.

2.8 Photocatalytic Reactions

In this study a cotton wool was used after loading with neat ZnO and Ag/ ZnO separately in a set of experiments for each case. The dimensions of this piece of cotton were 10 x 10 cm in a solution of 10 ppm in100 mL of the congo red dye as a model of simulated industrial wastewaters. Reactions were carried out in a homemade reactor as shown in Figure 2. The resultant mixture was stirred for a half of an hour in order to reach adsorption equilibrium at room temperature under air conditions. Then reaction mixture was irradiated with light from low pressure mercury lamp (150 watt) with continuous stirring. Periodically, a sample of 3 mL of reaction mixture was withdrawn and centrifuged and the absorbance was recorded at wavelength 495 nm.

Figure 2. Schematic description of the homemade photoreactor that used in photocatalytic degradation of CRD

3. Results and Discussion

3.1 PowderX-rays Diffraction (PXRD)

XRD patterns for neat and doped zinc oxide were studied by analyzing the used powder under scan with x-rays and the required patterns were obtained using Brag equation [(19)] as follows:

$$n\lambda = 2d \sin\Theta \quad (1)$$

Where n is the integer number that refers to the number times of the used wavelength (1,2,3 etc…), ʎ is the wavelength of the source of x-rays (1.54 Å), ɵ is the diffraction angle, and (d) is the distance between the successive layers in the desired crystal (Shuanghu, Maojun, Lujun, Xiaoliang, Mei, Mab, and Wenzhong, 2010). XRD patterns for bare ZnO and that doped with silver are shown in Figure 3.

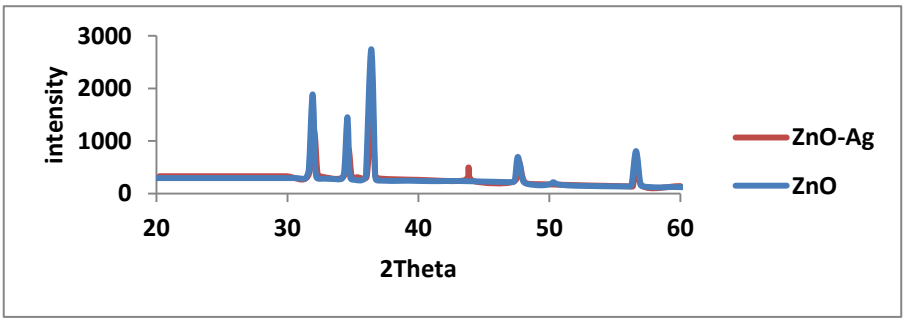

Figure 3. XRD patterns for neat ZnO and Ag/ZnO

From XRD patterns, it's possible to calculate values of lattice constants by considering ZnO as a hexagonal structure as shown in the following equation (Abbas, Salih, and Falah, 2008):

$$d=(a/\ ((3/4)\ (h^2 + k^2 + hk) + (a^2 / c)l^2))^{1/2} \quad (2)$$

Where, h, k, and l are miller constants and a, b, and c are the crystal lengths. The crystal size (D) was calculated using Scherre's equation (Bhatu, Lakhani, Tanna, Vasoya, Buch, Sharma, Trivedi, Joshi, and Modi, 200). These values are shown in Table. 1

$$D= 0.94\ \lambda/B\ Cos\theta \quad (3)$$

Where, θ is the diffraction angle, ʎ is the wavelength of the x-rays, and B is the full width at the half maxima.

Table 1. Diffraction angles and crystal size for neat and silver doped zinc oxide

Catalyst	2theta/deg	crystal size(nm)
ZnO	36.399	17.818
Ag/ZnO	36.440	29.106
Ag	34.830	6.722

From XRD patterns for neat and doped zinc oxide with silver, it's clear that doping ZnO with silver doesn't change its crystallinity as its shown from XRD patterns. The peaks for the oxide after doping with Ag are almost the same for the bare form. There was a weak new peak for the doped zinc oxide around (2Ɵ= 43º). This peak many be related to the presence of Ag particles on the surface of ZnO (Zdenek, Marta, Peter, Sarka, Martin, and Nicolas, 2012) . Silver particles have a nano-size of around 7 nm. This size probably facilitate the dispersion of Ag particles on the surface homogeneity without altering its crystal structure. Silver ions have ionic radius that is greater than zinc ion so that it can't introduce into the ZnO lattice and they can homogeneously distributed within ZnO matrix (Zdenek, Marta, Peter, Sarka, Martin, and Nicolas, 2012). So that doping ZnO with silver doesn't alter it crystal structure.

3.2 FTIR Spectra for Neat and Ag Doped Zinc Oxide

The functional groups for each neat zinc oxide and that doped with silver were studied using FTIR spectroscopy. The characteristic peak at 450 cm^{-1} is related to the stretching vibration mode for Zn-O bond in zinc oxide. FTIR spectra for neat and doped zinc oxide are shown in Figure 4.

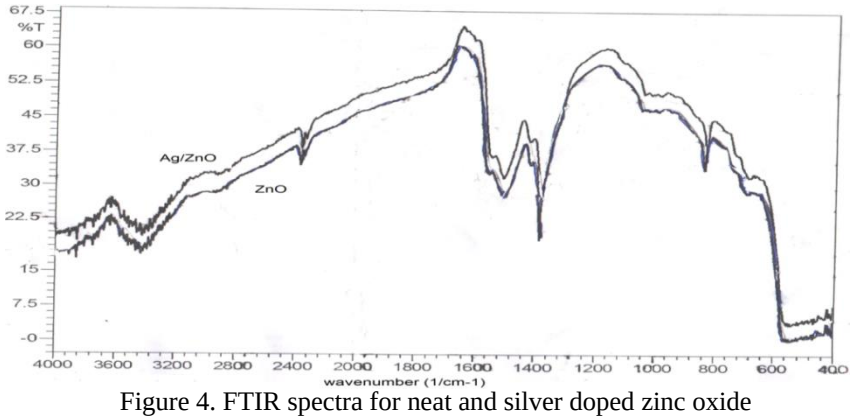

Figure 4. FTIR spectra for neat and silver doped zinc oxide

From above figure, it's clear that FTIR spectrum for Ag/ZnO is seemed to be similar to that for neat zinc oxide. In these spectra, the bands around 1630 cm^{-1} and that around 3436 cm^{-1} are correlated to the stretching modes of OH groups in these materials. The bands that are appeared at low frequencies around 450 and 590 cm^{-1} are assigned to the bending vibration of the characteristic peak for Zn-O bonds. Doping silver in these limits doesn't leads to appear further new peaks. This probably arises from homogeneous dispersion of Ag particles on the zinc oxide surface without formation any clusters (Mahmoudian, Basirum, Alias, and Khorsand, 2011). The band that appears around 3400 cm-1 is assigned to vibration mode of O-H group that are present in the catalyst. A weak band that appears around 2900 cm-1 is assigned to C-H modes. The Sharp band that appears around 1400-1600 cm-1 are assigned to stretching vibration modes for C=O groups. As our measurements were conducted under normal atmospheric conditions, so that bands that are appeared around 2350 cm-1 can be assigned to the presence of adsorbed CO_2 on the surface (Tas, Peter, Majewski, and Fritz, 2000).

3.3 Scanning Electron Microscopy (SEM)

Morphological study for both neat zinc oxide and that doped with silver was investigated using SEM. Morphologies of ZnO and Ag/ZnO are shown in Figure 5. From these images it can be concluded that, bare zinc oxide was relatively homogeneous and agglomerated, also it has an average particles size around (18 nm). This can be attributed to the uniform distribution of zinc cations in three dimensional structure (Falah, and Ahmed, 2007). The presence of these agglomerates is due to the densification that results due to the narrow space between particles. For zinc oxide doped with silver, the sample turned more homogeneous with relatively larger particle size around (29 nm) (Rauf, and Salman, 2009).

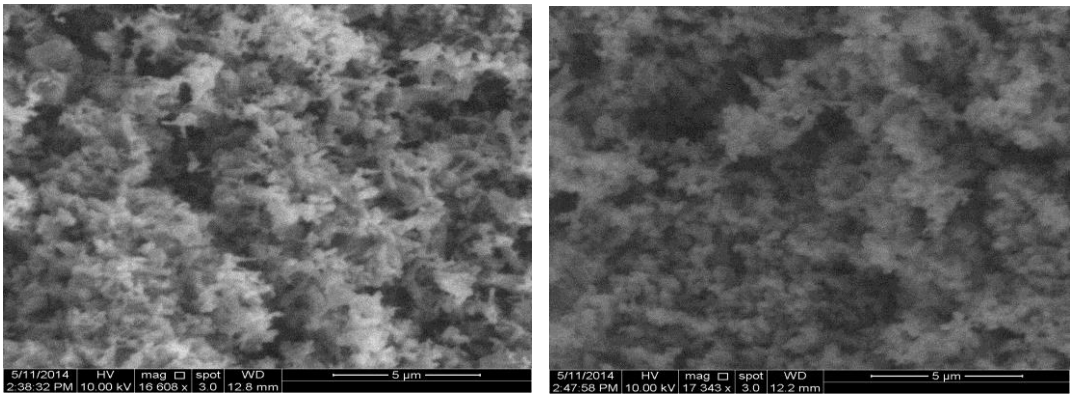

ZnO neat Ag/ZnO

Figure 5. SEM images for neat and silver doped zinc oxide

3.4 Photocatalytic Activity of Neat and Modified Zinc Oxide

3.4.1 Congo Red Dye Removal

The photocatalytic activity for each neat and doped zinc oxide and for the cotton loaded form was investigated by following congo red dye (CRD) removal from aqueous solution. From these results, it was found that dye removal using Ag/ZnO was more efficient than using bare zinc oxide under the same conditions. After three hours duration of reaction the percent of dye removal was 22% and 85% for each ZnO and Ag/ZnO respectively. High efficient activity for dye removal over silver doped zinc oxide probably arises from the reduction in the rate of recombination reaction which commonly occurs when use neat photocatalyst. This process can reduce the efficiency of the photocatalytic activity by the dissipation of excitation energy via recombination of e^-_{CB} and h^+_{VB} by back electron transfer (Himanshu, Hailemichael, Lebohang, Mantoa, Madhavi, and Gundu, 2009). The results of CRD removal for each of photolysis, adsorption, ZnO and Ag/ZnO are shown in Figure 6.

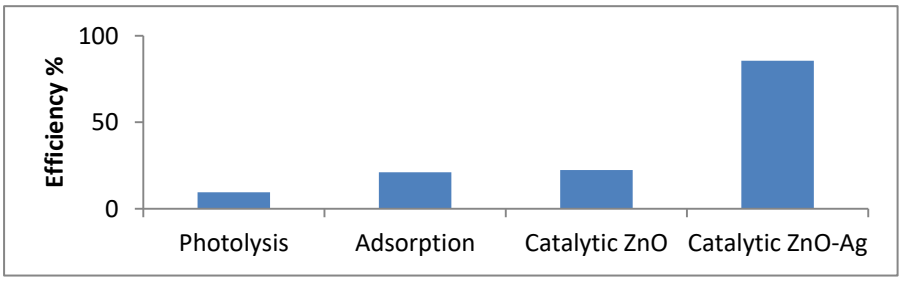

Figure 6. Removal of CRD from aqueous solution over neat and doped photocatalyst (error bar = ±2%)

The results of dye removal for loaded catalysts over cotton are shown in Figure 6. From these results, it was found that the photolysis of dye was not efficient and the rate constant for this process was 0. 6 x 10^{-3} min^{-1}. Also the adsorption process for the dye was more efficient of the removal of dye by photolysis and the rrate constant for adsorption was higher than the first case (0. 71 x 10^{-3} min^{-1}). Photocatalytic dye removal over cotton supported Ag/ZnO was more efficient than above two cases and the rate constant for this was 0. 74 x 10^{-2} min^{-1}. These results are shown in Figure 7.

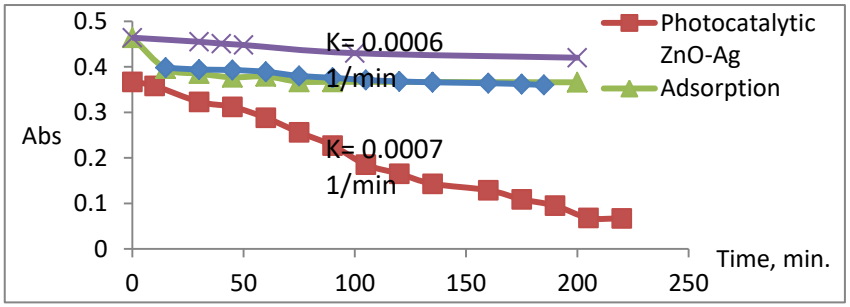

Figure 7. The removal of CRD over supported catalyst over on cotton texture

The presence of doped Ag particles on zinc oxide surface can increase its photocatalytic activity as these particles act as electronic collectors (sink for electrons). This can increase the rate of charge separation between e^-_{CB} and h^+_{VB} and consequently reduce recombination reaction (Sakthivela, Shankbar, Palanichamyb, Banumathi, Bahnemanna, and Murugesanb, 2004).

3.4.2 Effect of Light Intensity on Dye Removal

The effect of light intensity on the removal of CRD was investigated in this study by changing the separated distance between the source of light and the reaction mixture. The intensity of light is inversely proportional with the distance. Increasing of light intensity in this case can lead to increase the number of the photoexcited electrons. Higher light intensities can cause thermal quenching and then reduces number of excited electrons. On the other hand lower light intensities can lead to excite small number of particles of the photocatalyst which results in low photocatalytic activity at lower light intensities. The results of the effect of light intensity on CRD removal are shown in Figure 7. From these results it was found that the rate of the photodegradation of this dye was increased as the separated distances were reduced. These results are shown in Figure 8.

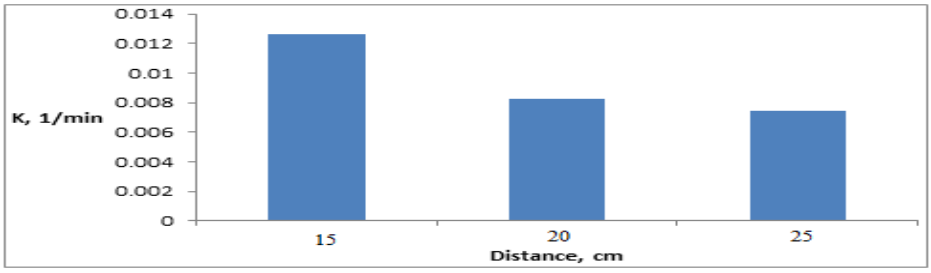

Figure 8. The effect of distance between source of light and the reaction mixture (error bar = $\pm 1 \times 10^{-4}$)

3.4.3 The Effect of Duration of Time on Dye Removal

Duration time of reaction is very important factor that can affect considerably on the efficiency of the reaction. Generally, there is a direct proportionality between the percentage of dye emoval and the time of illumination of reaction mixture (Ahmed, Abbas, Zahra, and Falah, 2014). For fully removal of CRD from aqueous solution took 2.5 hour , this was viewed by following the UV-Vis for this dye and the two peaks at 496 and 340 nm was decreased gradually with irradiation time. The effect of time of irradiation on dye removal is shown in Figure 9.

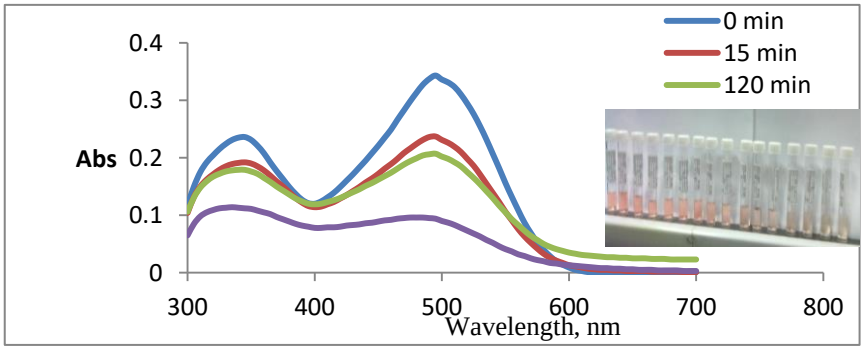

Figure 9. The effect of duration time on CRD removal from simulated wastewaters

3.4.4 Reproducibility of the Texture on the Catalysis Process

To show the ability of the cotton texture to be used as a carrier for the doped zinc oxide (Ag/ZnO), a series of experiments were performed by using the same carrier (texture) with Ag/ZnO in two batches. For each case the removal of CRD was recorded, from the obtained results, it was found that the activity of dye removal was reduced when used this catalyst in a second trial for the same irradiation time .gradually. After 120 minutes of irradiation the activity of dye removal was around 55% while in the second trial it was around 29%. The activity of the catalyst drops with times of usages due to the poisoning of the catalyst or due to the donation of some elements from the dye such as sulfur, this may react with zinc at the surface of the catalyst to form ZnS also it can react with silver to yield Ag_2S. For all these probabilities the catalyst suffers from poisoning and hence shows a lower activity with the further reproducibility. The results of two reproducibility are shown in Figure 10.

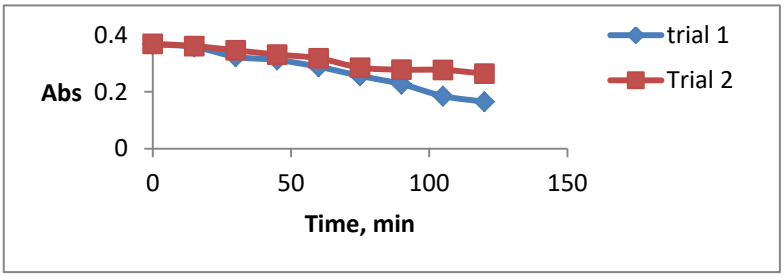

Figure 10. The reproducibility of the texture in CRD removal

3.4.5 Effect of pH on Dye Removal

Surfaces of oxides normally having unsaturated oxygen atoms, this possessing bonding deficiency and consequently are affected by basic/acidic environment. This differs depending on the type of atoms and crystal structure of the catalyst. According to this observation the surface of oxide in the reaction mixture would be either positive or negative depending on the abundance of H^+ and/or OH^-.

In acidic media the surface of oxide would have a positive charge while exhibits a negative charge under basic media as it is shown in the above equations. The surface of the catalyst exhibits a zero net charge of the surface at its point zero charge (PZC), for pH values lower than PZC surface has a positive charge while exhibit a net negative charge at pH values higher than its PZC. Generally PZC value for zinc oxide ranged from pH values (8-10). The results of the photocatalytic degradation was increased with increasing the value of pH towards basic values and the best esult was obtained around pH=9. Figure 11 shows the results of the dye removal under different pH values. From these results the efficiency of dye removal was enhanced in basic pH values and reduced in acidic values (Mirhadi, Tavangarian, and Emadi, 2012). By considering the rate constant for each pH value it was found that the rate of dye removal was affected considerably with the change in pH value of reaction mixture. The efficiency of dye removal was enhanced at pH values that are close to the PZC value and this arises from the surface charge neutralization at these range of pHs. This effect can minimize the repulsion forces between the surface and the adsorbed dye molecules on the surface. These results are shown in Figure 11.

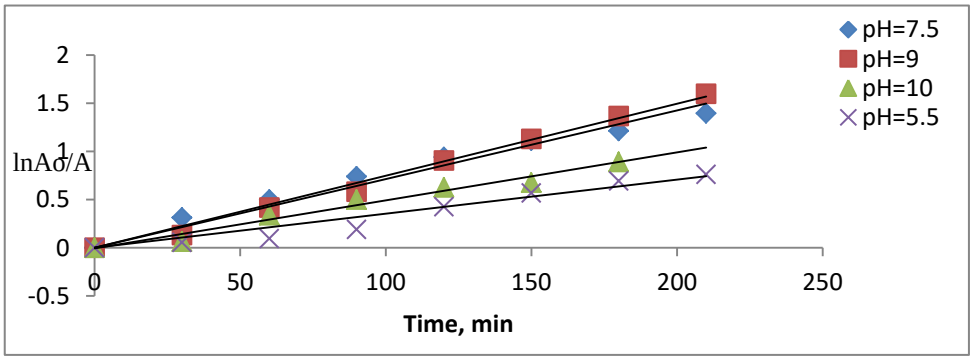

Figure 11. pH effects on the photocatalytic removal of CR dye over Ag/ZnO

3.4.6 Dye Removal from Cotton Texture

Cotton texture was immersed in the dye solution 10 ppm for 30 minutes with irradiation with mercury lamp with continuous stirring at room temperature. After complete dye removal from the aqueous solution and the initial

solution was turned colorless, irradiation was kept under the same conditions until the color was removed from the cotton texture completely (Tabrez, Singh, and Kumar, 2004). These observations are shown in Figure 12. From these results it's clear that this process can lead to remove the dye form the polluted clothes with the dyes by using irradiation only without need to use normal washing processes with using detergents (Sakthivel, Neppolian, Palanichamy, Arabindo, and Murugesan, 2000).

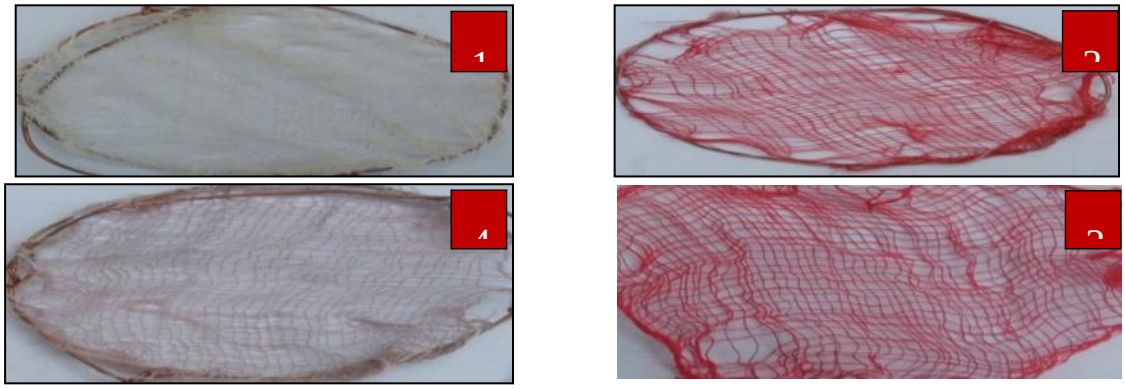

Figure 12. Images show decolorization of CR dye from the texture that is loaded initially with Ag/ZnO (1: Before adsorption process, 2: After dye adsorption, 3: Photocatalytic dye removal from the aqueous solution, and 4: The texture after being irradiated with mercury lamp

4. **Conclusions**

This study involves synthesis of a composite of Ag/ZnO with cotton texture by photodeposition method. Silver doped zinc oxide showed a higher activity in dye removal in comparison with un-doped oxide. Additionally the composite of Ag/ZnO/ texture showed a higher activity with respect to Ag/ZnO. The composite Ag/ZnO/ texture showed an ability towards self-cleaning of dye under irradiation. Also it was found that the activity of zinc oxide was increased in pHs ranges that are close to its point zero charge.

References

Abbas, J. A., Salih, H. K., & Falah, H. H. (2008). Photocatalytic Degradation of Textile Dyeing Wastewater Using Titanium Dioxide and Zinc Oxide, *E-Journal of Chemistry*, 5(2), 219-223, http://www.e-journals.net.

Agustin, R., Gonz âlez, E., & Javier, S. (1988). An electron spin resonance study of charge-carrier stabilization in ZnO. *J. Chem. Soc., Faraday Trans,. 1*, 84, 3961-3971. http://dx.doi.org/10.1039/f198884fx041

Ahmed, F. H., Abbas, J. A., Zahra, H. A., & Falah, H. H. (2014). Adsorption of Reactive Yellow Dye 145 from Wastewater ontoIraqi Zahdy and Khestawy Date Palm Seeds Activated Carbons, *Asian Journal of Chemistry., 26, Supplementary Issue (2014), S167-S172*, http://dx.doi.org/10.14233/ajchem.2014.19038

Alan, C., & Desmond, E. (1991). Ultraviolet–visible absorption spectra of the colloidal metallic elements, *J. Chem. Soc., Faraday Trans.*, 87, 3881-3891. DOI: 10.1039/FT99187FX093

Amy, L. r., Guangquan, L. , & John, T. Y. (1995). Photocatalysis on TiO_2 Surfaces: Principles, Mechanisms, and Selected Results, *Chem. Rev.*, *95*(3), 735–758, DOI: 10.1021/cr00035a013

Applications, *J. Phys., Condens. Matte*r, 16,829–858, PII: S0953-8984(04)58969-5

Au and Pd deposited on TiO2 catalyst, *Water Research*, 38, 3001–3008, www.elsevire/locate/waters.

Bahnemanna, D., & Murugesanb, V. (2004). Enhancement of photocatalytic activity by metaldeposition: characterisation and photonic efficiency of Pt

Bhatu, S., Lakhani, V., Tanna, A., Vasoya, N., Buch, J., Sharma, P., Trivedi, V., Joshi, H., & Modi, K. (2007). Effect of nickel substitution on structural infrared and elastic properties of lithium ferrite, *Indian Journal of Pure and Applied Physics*, *45*, 596-608. *nopr.niscair.res.in/bitstream/123456789/.../IJPAP%2045(7)%20596-608.pdf*

Falah, H. H., & Ahmed,A. J. (2007). Photo-oxidation of benzyl alcohol under natural weathering conditions, Desalination 209, 350–355, http://dx.doi.org/10.1016/j.desal.2007.04.050

Ghaed, M., Hossaini, S., & Ramezanis, S. (2012). Platinum Nanoparticles Loaded on Activated Carbonas Novel Adsorbent for the Removal of Congo Red, E-Journal of Chemistry, 9(1), 63-74. http://www.e-journals.net

2012

Gӧpel, W., Rocker, G., & Feierabend, R. (1983). Intrinsic defects of TiO2(110): Interaction with chemisorbed O2, H_2, CO, and CO_2. *Phys. Rev. B, 28*(6), 3427–3435. http://dx.doi.org/10.1103/PhysRevB.28.3427

Gunnar, A. Niklasson, G., & Claes, G. (2007). Electrochromics for smart windows: thin films of tungsten oxide and nickel oxide, and devices based on these. *J. Mater. Chem., 17*, 127-156. http://dx.doi.org/10.1039/B612174H

Hadjiivanov, K., Lamotte, J., & Lavalley, J. C. (1997). FTIR Study of Low-Temperature CO Adsorption on Pure and Ammonia-Precovered TiO_2 (Anatase). *Langmuir, 13*, 3374-3381. DOI: 10.1021/la962104m

Henglein, A. (1982). Photochemistry of colloidal cadmium sulfide. 2. Effects of adsorbed methyl viologen and of colloidal platinum. *J. Phys. Chem., 86*(13), 2291–2293, http://dx.doi.org/10.1021/j100210a010

Himanshu, N., Hailmichael A.. Lebohang, M., Mantoa, S., Madhavi, T., & Gundu, R. (2009). Role of particle size in visible light photocatalysis of Congo Red using TiO2·[ZnFe2O4]x nanocomposites *Bull. Mater. Sci*., *32*(5), 499–506. http://dx.doi.org/10.1007/s12034-009-0074-0

Hind, A., Bahaa, H. R., Hussein, H., Ahmed, H., & Saba, R. S. (2013). Preparation and Study of Optical Properties of (Polymer- Nickel Nitrate) Composite. *Advances in Physics Theories and Applications*, *20*, 152-157. www.iiste.org

Mahmoudian, M., Basirun, W., Alias, Y., & Khorsand, A. (2011). Electrochemical characteristics of coated steel with poly(N-methyl pyrrole)

Malinda, D., Reichert, D., Chia, L., & Javier, V. (2014). How Robust are Semiconductor Nanorods? Investigating the Stability and Chemical Decomposition Pathways of Photoactive Nanocrystals. *Chemistry of Materials*, *26*(13), 3900-3908. http://dx.doi.org/10.1021/cm500896n

Manoj, A. L., Shaji, V., & Santhosh, S. N. (2012). Photocatalytic Water Treatment by Titanium Dioxide: Recent Updates. *Catalysts, 2*, 572-601. http://dx.doi: 10.3390/Catal2040572.dx

Mirhadi, S., Tavangarian, F., & Emadi, R. (2012). Synthesis, characterization and formation mechanism of single-phase nanostructure bredigite powder, *Materials Science and Engineering C. Materials Science and Engineering C*, *32*, 133–139, http://dx.doi.org/10.1016/j.msec.2011.10.007

Narendra, T., Oza, A., & Ingale, S. (2014). TiO_2 as an Oxidant for Removal of Chemical Oxygen Demand from Sewage. *Universal Journal of Environmental Research and Technology*, *4*(3), 165-171. www.environmentaljournal.org

Noriyuki, S., Osamu, K. A., & Youkoh, K. (1995). Solvent effect on the photoinduced electron-transfer reactions between dicyanobis(polypyridine)ruthenium(II) complexes and tris(β-diketonato)ruthenium(III) complexes. *J. Chem. Soc., Faraday Trans., 91*, 437-443, http://dx.doi.org/10.1039/ft9959100437

Rajeev, J., & Shalini, S. (2008). Photodestruction and COD removal of toxic dyeerioglaucine by TiO2-UV process: influence of

Rauf, M., & Salman, S. (2009). Comparison of two different remediation methods for contaminated water treatment. *Aust. J. Ed. Chem., 70*, 42-48,

Rizzo, L., Meric, S., Guida, M., Kassinas, D., & Belgiorno, V. (2009). Heterogeneous Photocatalytic Degradation Kinetics and Detoxification of an Urban Wastewater Treatment Plant Effluent Contaminated with Pharmaceutical, Water Res., 43, 4070-4078. http://dx.doi.org/10.1016/j.watres.2009.06.046

Sakthivel, S., Neppolian, B., Palanichamy, M., Arabindoo, B., & Murugesan, V. (2000). ZnO/UV mediated photocatalytic degradationof Acid green 16, a commonly used leather dye. *Indian J. Eng. Mater Sc*i., *7*, 87–93.

Sakthivela, S., Shankarb, M., Palanichamyb, M., Banumathi, A., Santos, F. V., Azevedo, E. B., & Sant, Annar, G. L., & Dezottil, M. J. (2006). Photocatalysis as a Tertiarytreatment for Petroleums Refinery Wastewaters. *Brazilian Journal of Chemical Engineering*, *23*(4). 451 - 460, www.abeq.org.br/bjche

Shuanghu, H., Maojun, Z., Lujun, Y., Xiaoliang, Y., Mei, L., Li, M., & Wenzhong, S. (2010). Preparation and properties of ZnO nanostructures by electrochemicalanodization method, *Applied Surface Science*, *256*, 2557–2562, http://dx.doi.org/10.1016/j.apsusc.2009.10.104

Synthesized in presence of ZnO nanoparticles. *Thin Solid Films*, *520*, 258–265, www.elsevi e r.com/locate/tsf.

Tabrez, A., Singh, V., & Kumar, D. (2004). Removal of some basic dyes from artificial textile wastewater by

adsorption on akash kinari coal, *Journal of Scientific and Industrial Research*, *63*, 335-364

Tas, A. ¸Peter, M., & Fritz, A. (2000). Chemical Preparation of Pure and Strontium- and/or Magnesium-Doped Lanthanum Gallate Powders, *J. Am. Ceram. Soc.*, *83*(12), 2954–60. http://dx.doi.org/10.1111/j.1151-2916.2000.tb01666.x

Zdenek, M., Marta, H., Petr, S., Sarka, K., Martin, Z., & Nicolas, M. (2012). Photocatalytic Activity of Nanostructured Titanium Dioxide Thin Films. *International Journal of Photoenergy*, 1-8. http://dx.doi.org/10.1155/2012/689154

Zheng, M., Dillon, M., Eugen, P, Albert, V. D., Moneesh, U., & Latika, M. (2013). Vapor–liquid–solid growth of serrated GaN nanowires: shape selection driven by kinetic frustration. *J. Mater. Chem. C*, *1*(44), 7257–7460. www.rsc.org/MaterialsC